VOL. 5, NO. 5, May 2015 ISSN 2225-7217
ARPN Journal of Science and Technology

http://www.ejournalofscience.org

Impact of Heat Transfer on MHD Boundary Layer of Copper Nanofluid at a Stagnation Point Flow Past a Porous Stretching and Shrinking Surface with Variable Stream Conditions

[1] E N. Ashwin Kumar, [2] Norasikin Binti Mat Isa, [3] R. Kandasamy
[1,2] Faculty of Mechanical Engineering , [3] Faculty of Science, Technology and Human Development,
Research Centre for Computational Mathematics, University Tun Hussein Onn Malaysia, Johor, Malaysia
future990@gmail.com

ABSTRACT

In this paper, the effects of MHD boundary layer on a stagnation point flow and heat transfer over a porous stretching/shrinking surface in nanofluids are analyzed. The resulting system is then solved numerically by Maple 18 software. It is concluded that the magnetic field can be used as a means of controlling the heat transfer characteristics in the presence of copper nanofluid.

Keywords: *Copper nanofluid, porous medium, Stagnation-point flow, Thermal radiation, Magnetic field, Heat source /sink.*

NOMENCLATURE

C_p	specific heat at constant pressure
E_c	Eckert number
K	permeability of the porous medium
K^*	Roseland mean spectral absorption coefficient
N	thermal radiation parameter
Pr	Prandtl number
q_r	thermal radiative heat flux
Q_0	dimensional heat generation/absorption coefficient
$\mathrm{Re}\,x$	local Reynolds number
S	suction/injection parameter
T	temperature of the fluid
T_∞	free stream temperature
T_w	temperature at the wall
u	velocity component in x-direction
u_w	stretching/shrinking sheet velocity
U	free stream velocity of the nanofluid
V	velocity component in y-direction
x, y	direction along and perpendicular to the plate, respectively

Greek symbols

α_{nf}	effective thermal diffusivity of the nanofluid
α_f	fluid thermal diffusivity
ζ	solid volume fraction of the nanoparticles
η	similarity variable
λ	heat generation/absorption parameter
μ_{nf}	effective dynamic viscosity of the nanofluid
μ_f	dynamic viscosity of the fluid
ν_f	kinematic viscosity of the fluid
ρ_{nf}	effective density of the nanofluid
σ^*	Stefan–Boltzmann constant
θ	dimensionless temperature of the fluid
θ_w	wall temperature excess ratio parameter
ψ	stream function
κ_{nf}	effective thermal conductivity of the nanofluid
κ_f	thermal conductivity of the fluid

1. INTRODUCTION

An innovative way to increase conductivity coefficient of the fluid is to suspend solid nanoparticles in it and make a mixture called nanofluid, having larger thermal conductivity coefficient than that of the base fluid. This higher thermal conductivity enhances the rate of heat transfer in industrial applications. Many researchers have investigated different aspects of nanofluids and have paid much attention to viscous fluid motion near the stagnation region of a solid body, where "body" corresponds to either fixed or moving surfaces in a fluid. This multidisciplinary flow has frequent applications in high speed flows, thrust bearings, and thermal oil recovery. All studies mentioned above refer to the stagnation-point flow towards a stretching/shrinking sheet in a viscous and Newtonian fluid. Most conventional heat transfer fluids, such as water, ethylene glycol, and engine oil, have limited capabilities in terms of thermal properties, which, in turn, may impose serve restrictions in many thermal applications. On the other hand, most solids, in particular, metals, have thermal conductivities much higher, say by one to three orders of magnitude, compared with that of liquids. Stagnation point flow is continuing to be an interesting area of research among scientists and investigators due to its importance in a wide variety of applications both in industrial and scientific applications. Some of the

applications are cooling of electronic devices by fans, cooling of nuclear reactors during emergency shutdown, solar central receivers exposed to wind currents, and many hydrodynamic processes in engineering applications.

Magneto hydrodynamic (MHD) boundary layer flow is of considerable interest in the technical field due to its frequent occurrence in industrial technology and geothermal application, high-temperature plasmas applicable to nuclear fusion energy conversion, liquid metal fluids and (MHD) power generation systems. The effect of thermal radiation on flow and heat transfer processes is of major importance in the design of many advanced energy conversion systems operating at high temperature. Thermal radiations within such systems occur because of the emission by the hot walls and working fluid. The process of fusing of metals in an electrical furnace by applying a magnetic field and the process of cooling of the first wall inside a nuclear reactor containment vessel where the hot plasma is isolated from the wall by applying a magnetic field are some examples of such fields.

The main subject of the present study is to study the two-dimensional Magneto hydrodynamic (MHD) boundary layer of stagnation-point flow in a nanofluid in the presence of thermal radiation. Using a similarity transform the Navier-Stokes equations have been reduced to a set of nonlinear ordinary differential equations. The resulting nonlinear system has been solved numerically using the Maple 18 software technique. Finally, the results are reported for two different types of nanoparticles namely alumina and copper with water as the base fluid. Nanofluids could be used in major process industries, including materials and chemicals, food and drink, oil and gas, paper and printing, and textiles. Nanofluids, when used as coolants can provide dramatic improvements in the thermal conductivity of host fluids compared to that of the traditional fluids. By using nanofluids highest possible thermal properties at the smallest possible concentrations by uniform dispersion and stable suspension of nanoparticles in base fluids can be achieved. Xuan and Li [1] used pure copper particles in the study of convective heat transfer and flow features of nanofluids. A comprehensive survey of convective transport in nanofluids was made by Buongiorno [2], who gave an explanation for the abnormal increase of the thermal conductivity of nanofluids. Therefore, by mixing the nanoparticles in the fluid, thermal conductivity of the fluids improve the heat transfer capability. Pantzali et al. [3] presented an experimental study that showed the role of CuO–water nanofluids as coolant in the plate heat exchangers. Recently, an analysis has been carried out by Vajravelu et al. [4] to study the convective heat transfer in a nanofluid flow over a stretching surface. In particular, they have focused on Ag–water and Cu–water nanofluids to investigate the effects of the nano particle volume fraction on the flow and heat transfer characteristics in the presence of thermal buoyancy and temperature-dependent internal heat generation/absorption. The thermal radiation effects become intensified at high absolute temperature levels due to basic difference between radiation and the convection and conduction energy-exchange mechanisms. A comprehensive review of the literature about stagnation point flow of nanofluids is given by references from [5–14]. Despite several works have been reported on flow and heat transfer of nanofluids, there seems to be no attempts in literature to consider the combined effects of buoyancy force and convective heating on hydro magnetic stagnation point flow and heat transfer of nanofluid towards a stretching / shrinking surface.

2. MATHEMATICAL ANALYSIS

Consider the steady two-dimensional stagnation-point laminar flow of a viscous nanofluid past a stretching / shrinking plate with linear velocity $u_w(x) = c\,x$ (for stretching sheet) / $u_w(x) = -c\,x$ (for shrinking sheet) and the velocity of free stream flow $U(x) = a\,x$ in the presence of magnetic field and the thermal radiation, where a and c are constants. The uniform magnetic field of strength B_0 is applied in the positive direction of x-axis.

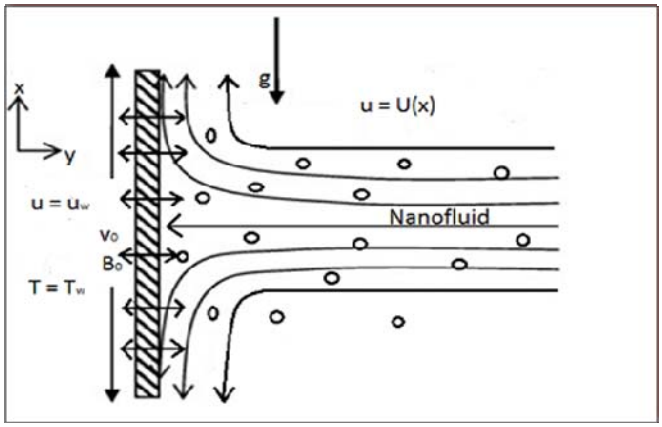

Fig 1: Physical flow model over a porous wedge sheet

The ambient uniform temperature of nanofluid is T_∞ where the body surface is kept at a constant temperature T_w (Fig. 1). It is assumed that the base fluid and nanoparticles are in thermal equilibrium and no slip occurs between them. Under these assumptions, the governing equations for the continuity, momentum and energy in boundary layer flow can be written as

$$\frac{\partial \overline{u}}{\partial \overline{x}} + \frac{\partial \overline{v}}{\partial \overline{y}} = 0 \qquad (1)$$

$$u\frac{\partial u}{\partial x}+v\frac{\partial u}{\partial y}=U\frac{dU}{dx}+\frac{\mu_{f_n}}{\rho_{f_n}}\frac{\partial^2 u}{\partial y^2}+\left(\frac{\mu_{f_n}}{\rho_{f_n}K}+\frac{\sigma B_0^2}{\rho_{f_n}}\right)(U-u)+g(T-T_\infty) \quad (2)$$

$$u\frac{\partial T}{\partial x}+v\frac{\partial T}{\partial y}=\alpha_{f_n}\frac{\partial^2 T}{\partial y^2}+\frac{Q_0(T-T_\infty)}{(\rho c_p)_{f_n}}-\frac{1}{(\rho c_p)_{f_n}}\frac{\partial q_r}{\partial y}+\frac{\mu_{f_n}}{(\rho c_p)_{f_n}}\left(\frac{\partial u}{\partial y}\right)^2 \quad (3)$$

with boundary conditions (for stretching / shrinking sheet)

$$u=u_w(x)=\pm,v=v_0,T=T_w=T_\infty+b\frac{x}{l}$$

at y = 0;

$$u\to U(x)=ax,v=0,T\to T_\infty \text{ as } y\to\infty \quad (4)$$

where '+' stands for stretching sheet and '−' for shrinking sheet in (4) for momentum field, u and v are the velocity components along the x and y directions, respectively. U (x) stands for the stagnation-point velocity in the in viscid free stream. T- temperature of the nanofluid, K- permeability of the porous media, Q_0 - heat generation or absorption coefficient, a , b and c are positive constants and v_0 - wall mass flux with $v_0>0$ for suctions and $v_0<0$ for injection, respectively. Further ρ is the fluid density, μ_{fn} is the coefficient of viscosity of the nanofluid, k_{fn} is the thermal conductivity of the nanofluid, α_{fn} is the thermal diffusivity of the nanofluid, ρ_{fn} is the effective density of the nanofluid, $(\rho c_p)_{fn}$ is the heat capacitance of the nanofluid, which is defined as follows:

$$\rho_{f_n}=(1-\zeta)\rho_f+\zeta\rho_s,$$

$$\mu_{f_n}=\frac{\mu_f}{(1-\zeta)^{2.5}},(\rho\beta)_{f_n}=(1-\zeta)(\rho\beta)_f+\zeta(\rho\beta)_s,$$

$$\alpha_{f_n}=\frac{k_{f_n}}{(\rho c_p)_{f_n}},$$

$$(\rho c_p)_{f_n}=(1-\zeta)(\rho c_p)_f+\zeta(\rho c_p)_s,$$

$$\frac{k_{f_n}}{k_f}=\left\{\frac{(k_s+2k_f)-2\zeta(k_f-k_s)}{(k_s+2k_f)+2\zeta(k_f-k_s)}\right\} \quad (5)$$

where ζ is the solid volume fraction of the nanofluid, ρ_f is the reference density of the fluid fraction, ρ_s is the reference density of the solid fraction, μ_f is the viscosity of the fluid fraction, k_f is the thermal conductivity of the fluid, and k_s is the thermal conductivity of the solid fraction.

We now look for a similarity solution of the Eqs. (1)-(3) with boundary conditions (4) in the following form:

$$\psi=\sqrt{c\nu_f}\ f(\eta)\,x,\theta(\eta)=\frac{T-T_\infty}{T_w-T_\infty},\eta=\sqrt{\frac{c}{\nu_f}}y \quad (6)$$

where ν_f is the kinematic viscosity of the fluid. The radiation heat flux is given as $q_r=-\frac{4\sigma^*}{3K^*}\frac{\partial T^4}{\partial y}$

where σ^* is Stefan–Boltzmann constant and K^* is the Roseland mean spectral absorption coefficient.

$$T^4=T_\infty^4\{1+(\theta_w-1)\theta\}^4 \quad (7)$$

where $\theta_w=\frac{T_w}{T_\infty}$ is the wall temperature excess ratio parameter. Defining the stream function ψ in the usual way such that $u=\frac{\partial\psi}{\partial y},,v=-\frac{\partial\psi}{\partial x}$ which identically satisfies the Eq. (1) and the equations (1)-(3) take the non-dimensional form

$$f'''+\left((1-\zeta)^{2.5}M+K_1\right)\left(\frac{a}{c}+f'\right)++(1-\zeta)^{2.5}\left(1-\zeta+\zeta\frac{\rho_s}{\rho_f}\right)\left(\frac{a^2}{c^2}+f\ f''-f'^2+Gr\theta\right)=0 \quad (8)$$

$$\frac{1}{\Pr}\left[\left(\frac{K_{fn}}{K_f}+N\{1+(\theta_w-1)\theta\}^3\right)\theta'\right]' + \left(1-\zeta+\zeta\frac{(\rho c_p)_s}{(\rho c_p)_f}\right)\left(f\theta'-2f'\theta\right)+\lambda\theta+\frac{Ec}{(1-\zeta)^{2.5}}f''^2=0 \quad (9)$$

with boundary conditions (for stretching / shrinking sheet)

$f = S,\ f' = 1, \theta = 1$ *at* $\eta = 0$ (*for stretching sheet*)
$f = S,\ f' = -1, \theta = 1$ *at* $\eta = 0$ (*for shrinking sheet*)

at y = 0;

$$f' \to \frac{a}{c}, \theta \to 0,\ \eta \to \infty \quad (10)$$

where $\lambda = \frac{Q_o}{(\rho c_p)_f}$ is the heat source ($\lambda > 0$) or sink ($\lambda < 0$) parameter, $K_1 = \frac{\nu_f}{c\,K}$ is the porous parameter, $S = \frac{v_o}{\sqrt{c\,\nu_f}}$ is the mass flux parameter ($s > 0$ corresponds to the suction and $s < 0$ corresponds to injection), $M = \frac{\sigma B_0^2}{c\rho_f}$ is the magnetic parameter, $Ec = \frac{u_w^2\,\mu_f}{K_{fn}\nabla T}$ is the Eckert number, $\Pr = \frac{\nu_f}{\alpha_f}$ is the Prandtl number, $N = \frac{16\sigma^* T^3}{3\,k_f K^*}$ be the radiation parameter and $\gamma = \frac{Gr}{\mathrm{Re}^2}$ is the buoyancy parameter, where $Gr = \frac{g\beta(T_w - T_\infty)}{c\,u_w}$ be the Grash of number, $\mathrm{Re} = \frac{u_w x}{\nu}$ be the Reynolds number. Here prime denotes the differentiation with respect to η .For practical purposes, the functions $f(\eta)$ and $\theta(\eta)$ allow us to determine the skin friction coefficient

$$C_f = \frac{2\mu_{f\,n}}{\rho_f u_w^{\,2}}\left(\frac{\partial u}{\partial y}\right)_{at\ y=0} = -\frac{1}{(1-\zeta)^{2.5}}(\mathrm{Re}\,x)^{-\frac{1}{2}} f''(0) \quad (11)$$

and the Nusselt number

$$Nu_x = \frac{x k_{f_n}}{k_f (T_w - T_\infty)}\left(\frac{\partial T}{\partial y}\right)_{at\ y=0} = -(\mathrm{Re}\,x)^{\frac{1}{2}}\frac{k_{f_n}}{k_f}\theta'(0)\left[1+\frac{4}{3}N(C_T+\theta(0))^3\right] \quad (12)$$

respectively. Here, $\mathrm{Re}_x = \frac{u_w\,x}{\nu_f}$ is the local Reynolds number.

3. RESULTS AND DISCUSSION

The set of equations (8) and (9) is highly nonlinear. Hence coupled and cannot be solved analytically and numerical solutions subject to the boundary conditions (10) are obtained using the very robust computer algebra software Maple 18. This software uses a fourth-fifth order Runge–Kutta–Fehlberg method as default to solve boundary value problems numerically using the dsolve command. For the benefit of the readers the Maple worksheet is listed in Appendix A. The transformed system of coupled nonlinear ordinary differential Equations (8) and (9) including boundary conditions (10) depend on the various parameters. The numerical results are represented in the form of the dimensionless velocity and temperature. During computation we choose parameter such that Pr = 6.2, correspond physically to air (nanofluid). In Table 2, the present results of $-\theta'(0)$ our compared with those of Mahapatra& Gupta [17] and Hamad & Pop [16]. The results show a very good agreement with their results as seen from the calculated percentage of errors since the errors are found to be very less. This may be due to the fact that we have used Runge–Kutta–Fehlberg method which has fifth-order accuracy. Thus the present results are more accurate than their results.

Table 1: Thermo physical properties of fluid and nanoparticles (Oztop and Abu-nada [15])

Physical properties	Fluid phase (water)	Cu	Al_2O_3	TiO_2
C_p (J/kg K	4179	385	765	686.2
ρ (kg/m^3)	997.1	8933	3970	4250
κ (W/m K)	0.613	400	40	8.9538

Table 2: Comparison of result for $-\theta'(0)$ in isothermal case when $\lambda = \phi = K_1 = Nr = Ec = b = 0$ for stretching sheet

Pr	a / c	Mahapatra and Gupta [17]	Hamad and Pop [16]	Present results
1	0.1	0.625	0.6216	0.625376218
	1.0	0.796	0.8001	0.799672174
	2.0	1.124	1.1221	1.123758921
1.5	0.1	0.797	0.7952	0.795008726
	1.0	0.974	0.7952	0.795036718
	2.0	1.341	1.3419	1.340956236

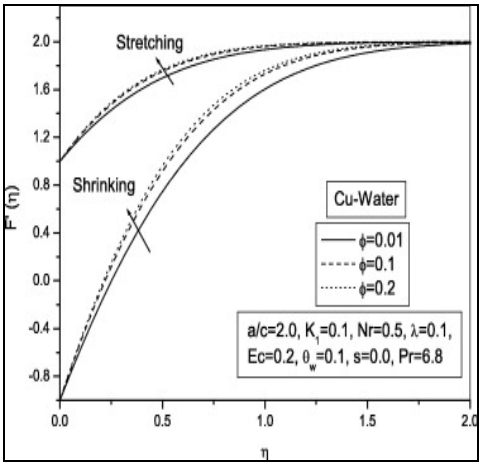

Fig 2(a): Dulal Pal et al. [18]

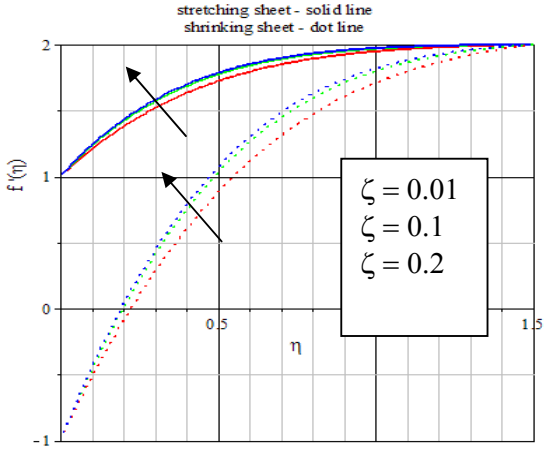

Fig 2(b): Present Result

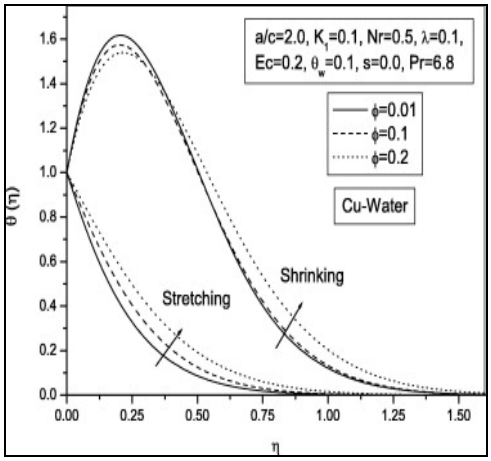

Fig 2(c): Dulal Pal et al. [18]

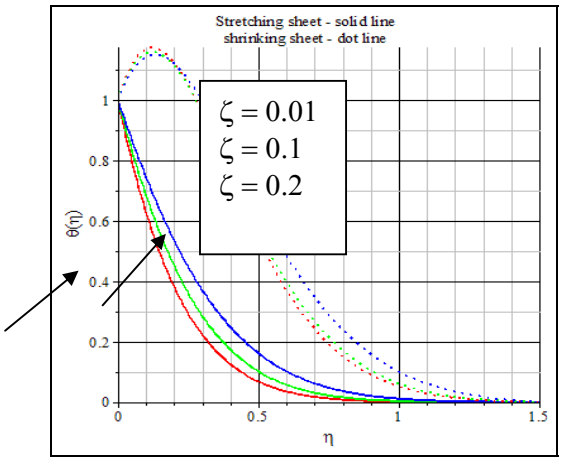

Fig 2(d): present result

Figs 2(a)-2(d): Nano particle volume fraction on the velocity and temperature field-comparison with Dulal Pal et al. [18]

It is also observed from the Figs. 2(a) – 2(d) that the agreement with the theoretical solution of velocity profile Fig.2(b) and temperature profile Fig. 2(d) for different values of □is excellent compared with Fig.2(a) and Fig.2(c) of Dulal Pal et al. [18] respectively.

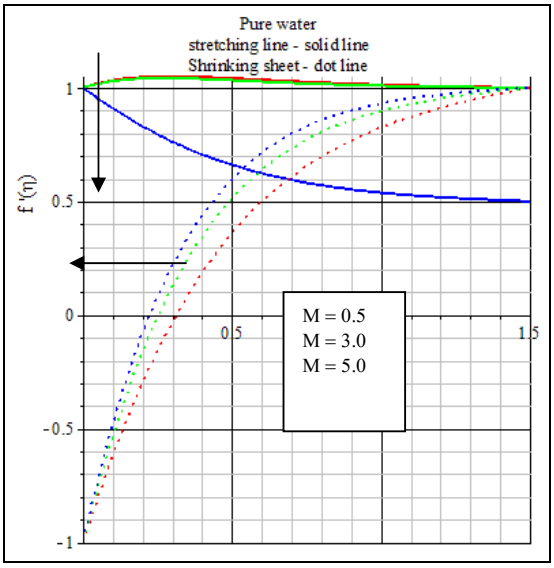

Fig 3(a)

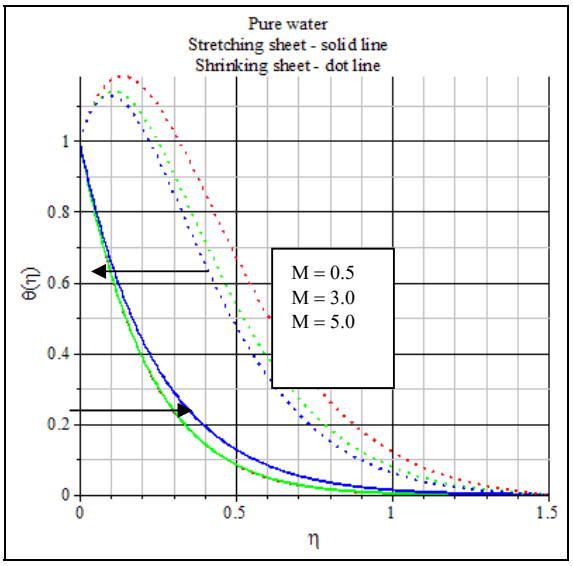

Fig 3(b)

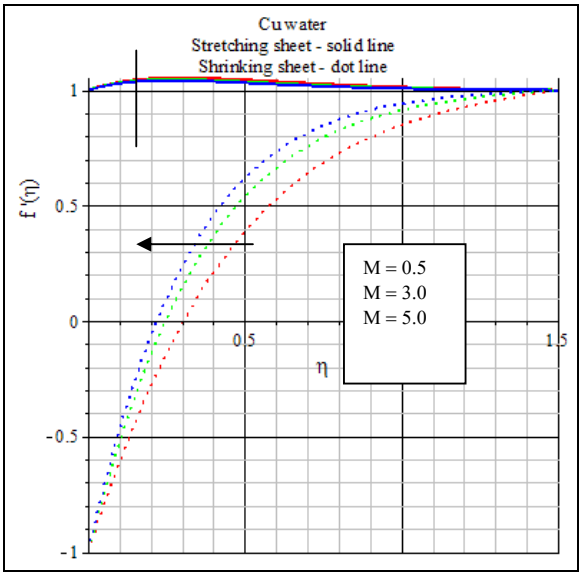

Fig 3(c)

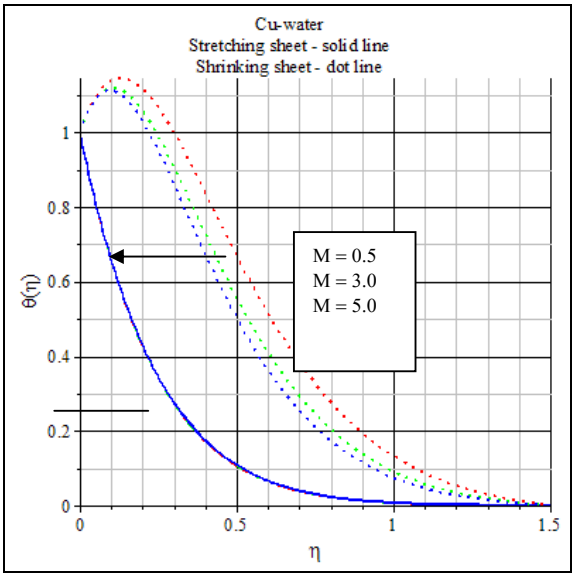

Fig 3(d)

Figs 3(a)-3(d): present typical profiles for velocity and temperature for different values of magnetic strength

In the presence of pure water(Figs. 3(a) and 3(b)),it is clearly shown that the velocity of the fluid decreases for stretching sheet and increases for shrinking sheet whereas the temperature of the fluid increases for stretching sheet and decreases for shrinking sheet with increase of magnetic strength, which implies that the applied magnetic field tends to heat the fluid and enhances the heat transfer from the wall for stretching sheet while the opposite reaction are shown for shrinking sheet. In the presence of copper nanofluid (Figs. 3(c) and 3(d)), the velocity of the fluid is uniform for stretching sheet and increases for shrinking sheet whereas the temperature of the fluid is uniform for stretching sheet and decreases for shrinking sheet with increase of magnetic strength.

As it move away from the plate, the effect of M becomes less pronounced. The effects of a transverse

magnetic field to an electrically conducting fluid gives rise to a resistive-type force called the Lorentz force. The Lorentz force clearly indicates that the transverse magnetic field opposes the transport phenomena and it has the tendency to slow down the motion of the fluid and to accelerate its temperature profiles for stretching sheet and the opposite effects are observed for shrinking sheet in the presence of pure water. Due to the copper nanofluid, it is interesting to note that velocity and temperature of the copper nanofluid for stretching sheet are uniform while the velocity increases and temperature of the nanofluid decreases for shrinking sheet. It implies that the strength of the magnetic field on copper nanofluid play a dominant role on shrinking sheet as well as on stretching sheet. In all cases, the temperature vanishes at some large distance from the surface of the vertical plate.

This result qualitatively agrees with the expectations, since magnetic field exerts retarding force on the natural convection flow. Physically, it is interesting to note that the changes on velocity and temperature of the copper nanofluid (Cu-Water) and base fluid significantly for shrinking sheet as compared to that of the stretching sheet because of the thermal conductivity of the nanofluids. Copper nano particle is a unique material that has both the liquid and magnetic properties. Many of the physical properties of these fluids can be tuned by varying magnetic field. These results clearly demonstrate that the magnetic field can be used as a means of controlling the flow and heat transfer characteristics.

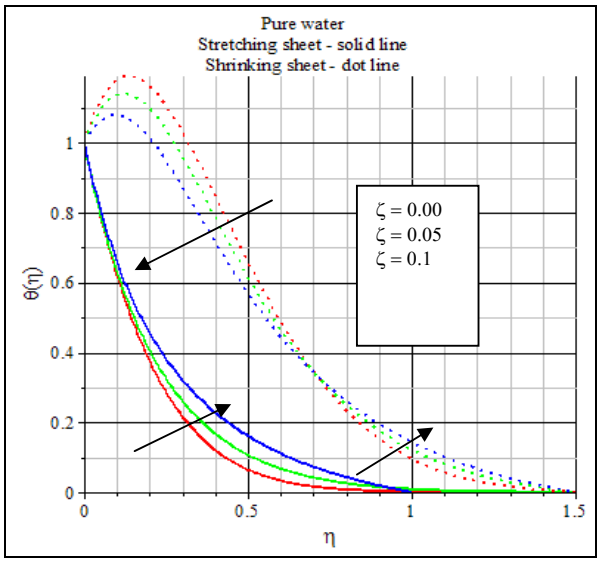

Fig 4(a)

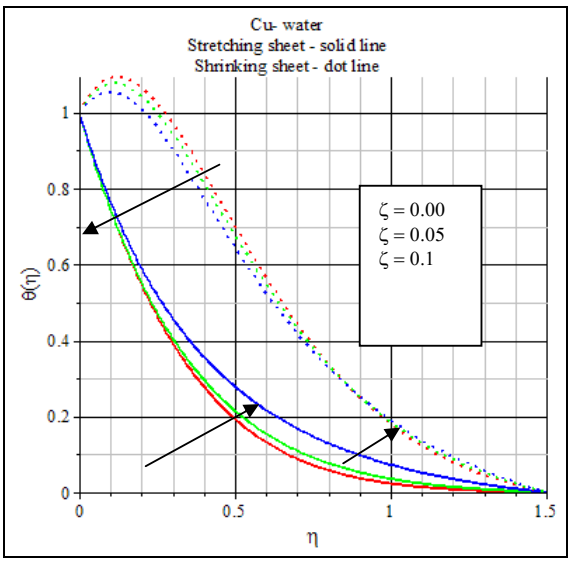

Fig 4(b)

Figs 4(a)-4(b): present the temperature profiles for different values of nano particle volume fraction

Figs. 4(a) and 4(b) predict the characteristic temperature profiles for different values of the nano particle volume fraction ζ for stretching and shrinking sheet in the presence of base fluid (pure water) and nanofluid (Cu-water). In both the cases (pure water and copper nanofluid), it is note that the temperature of the fluid accelerates for stretching surface with increase of ζ and there is a significance changes between them. For shrinking sheet, it is interesting to note that the temperature of the fluid decreases within the thermal boundary layer region $\eta < 0.715$ while outside $\eta \geq 0.715$, the temperature profiles gradually increases with increase of ζ for pure water whereas the temperature of the fluid decreases within the thermal boundary layer region $\eta < 0.845$ while outside $\eta \geq 0.845$, the temperature profiles gradually increases with increase of ζ for copper nanofluid because of high thermal conductivity of the copper nanofluid compared to that of base fluid. Further, it is noticed that values of the temperature profiles of ζ and tends to zero when $\eta = 1.12$ and $\eta = 1.53$ for stretching and shrinking sheets, respectively for pure water whereas the temperature of ζ coincide and tends to zero when $\eta = 1.51$ and $\eta = 1.67$ for stretching and shrinking sheets, respectively for Cu-water. It is important to note that the values of temperature profiles for shrinking sheet is more pronounced than the temperature profiles for the stretching sheet for pure and copper nanofluid. This is due to the fact that thermal boundary layer thickness changes with change in nano particle volume fraction strength ζ present in the Cu-water. Thus it is an evident that the formation of peak in the temperature profile for shrinking sheet is due to the fact the thermal boundary layer increases in this case whereas no peak formation is observed in the case of stretching sheet as thermal boundary layer is less than the

shrinking sheet for all the values of nano particle volume fraction. It is important to note that the increase of ζ for shrinking sheet plays a dominant role on temperature profiles compared to that of stretching sheet. This is in agreement with the physical fact that the thermal boundary layer thickness decreases with increasing nano particle volume fraction, ζ.

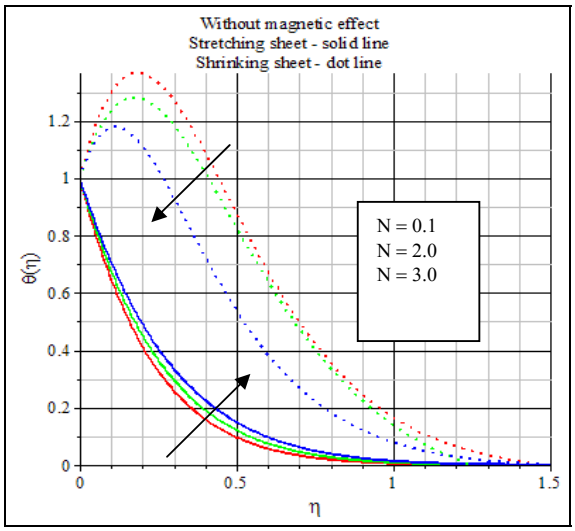

Fig 5(a)

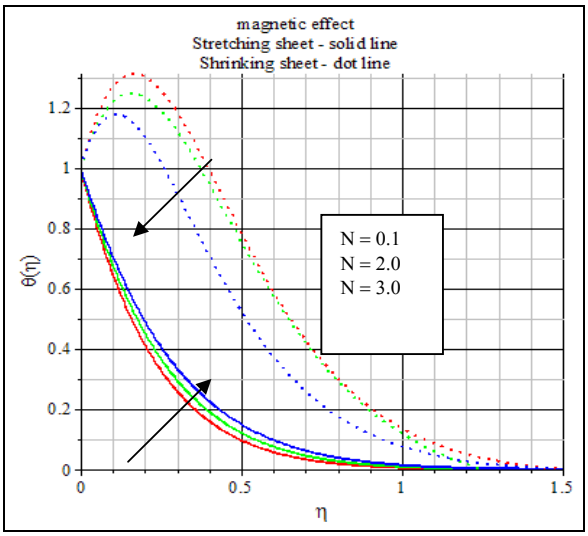

Fig 5(b)

Figs 5(a)-5(b): Present the temperature profiles for different values of thermal radiation

Figs. 5(a) and 5(b) display the effects of thermal radiation on the temperature distribution with or without magnetic field. In the presence of magnetic and non-magnetic field, it is note that the temperature of the fluid enhances with increase of N for stretching sheet whereas it decreases with increase of N for shrinking sheet. The sensitivity of thermal boundary layer thickness with N is related to the increased thermal conductivity of the nanofluid. Both the cases (with or without magnetic field), it is observed that the temperature of the nanofluid decreases with increase of N for shrinking sheet. In fact, higher values of thermal conductivity are accompanied by higher values of thermal diffusivity. It is important to note that the values of temperature profiles for shrinking sheet is more pronounced than the temperature profiles values for the stretching sheet. This is due to the fact that thermal boundary layer thickness changes with change in the type of nanoparticles present in the base fluid (water).

The high value of thermal diffusivity causes a drop in the temperature gradients and accordingly increases the boundary thickness as demonstrated in Fig. 5(b). This agrees with the physical behavior that when the volume fraction of copper nanofluids in the presence of magnetic field raises the thermal conductivity and then the thermal boundary layer thickness increases. Enhancement in thermal conductivity can lead to efficiency improvements, although small, via more effective fluid heat transfer. In general nanofluids show many excellent properties promising for heat transfer applications. Despite many interesting phenomena described and understood there are still several important issues that need to be solved for practical application of nanofluids with magnetic field. For stretching sheet, temperature profile gradually decreases with η whereas for shrinking sheet there is a formation of a peak near $\eta = 0.25$ which gradually increases linearly thereafter till the value of temperature goes to zero as $\eta \to 1.25$ for stretching sheet and $\eta \to 1.75$ for shrinking sheet (matching the boundary condition $\theta \to 0$ as $\eta \to \infty$). Thus it is an evident that the formation of peak in the temperature profile for shrinking sheet is due to the fact the thermal boundary layer increases in this case whereas no peak formation is observed in the case of stretching sheet as thermal boundary layer is less than the shrinking sheet for all the values of N. It is important to note that the temperature profile for shrinking sheet is higher compared to that of stretching sheet.

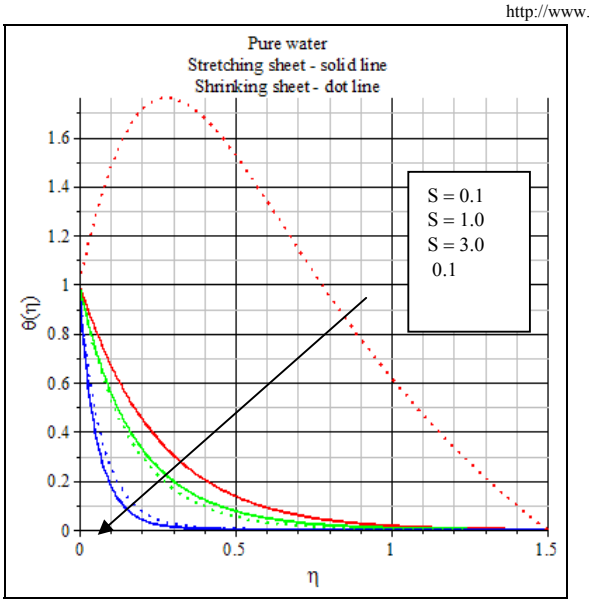

Fig 6(a)

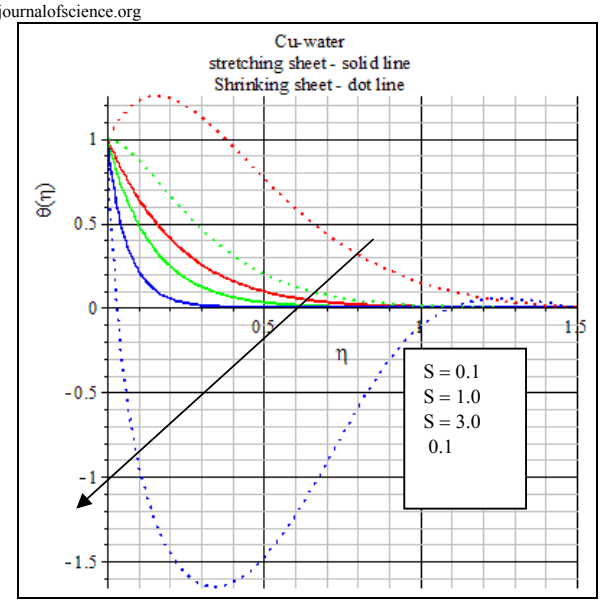

Fig 6(b)

Figs 6(a)-6(b): present the temperature profiles for different values of suction parameter

Figs. 6(a) – 6(b) depict the influence of the suction s on the temperature profiles in the boundary layer when the magnetic strength is uniform, i.e. $M = 0.5$, in the case of pure and Cu-water for stretching and shrinking sheet respectively. It is observed that the temperature in the boundary layer decreases with the increase of suction parameter (S > 0). The explanation for such behavior is that the fluid is brought closer to the surface and reduces the thermal boundary layer thickness in case of suction. As such then the presence of wall suction decreases the thermal boundary layer thickness, i.e. thins out the thermal boundary layer in the nanofluid Cu-water as well as pure water. It is interesting to note that the temperature of the fluid gradually changes from higher value to lower value only when the strength of suction parameter higher than the magnetic strength in the presence of Cu-water for shrinking sheet. For heat transfer characteristics mechanism for shrinking sheet, interesting result is the large distortion of the temperature field caused for $S \geq 3$ because of high thermal conductivity of the copper nanofluid. Negative value of the temperature profile for shrinking sheet is seen in the outer boundary region for $S = 3$. The decrease in thickness of the temperature layer was caused in two ways: (i) the direct action of suction, and (ii) the indirect action of suction causing a thicker thermal boundary layer which corresponded to a lower temperature gradient, a consequent increase in the buoyancy force and a higher temperature gradient. However, the exact opposite behavior is produced by imposition of wall fluid blowing or injection. It is note that, for particular value of M and at each position, the corresponding value of the temperature in the presence of nanoparticles is smaller than the value of the temperature for basic fluid. All these physical behavior are due to the combined effects of the strength of magnetic effect in the presence volume fraction of the nanoparticles.

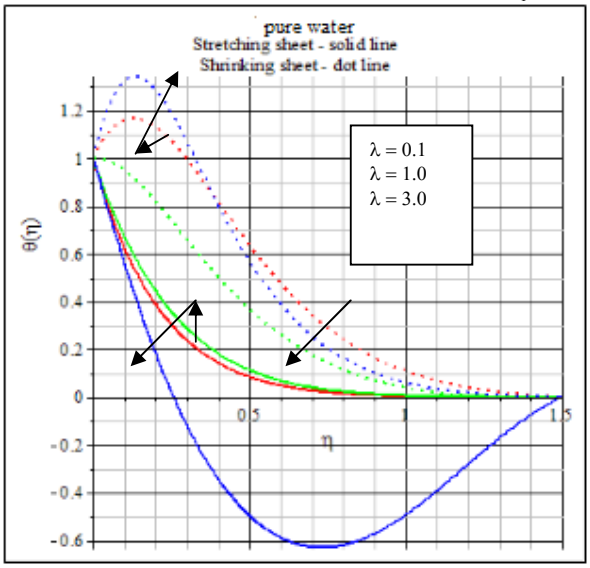

Fig 7(a)

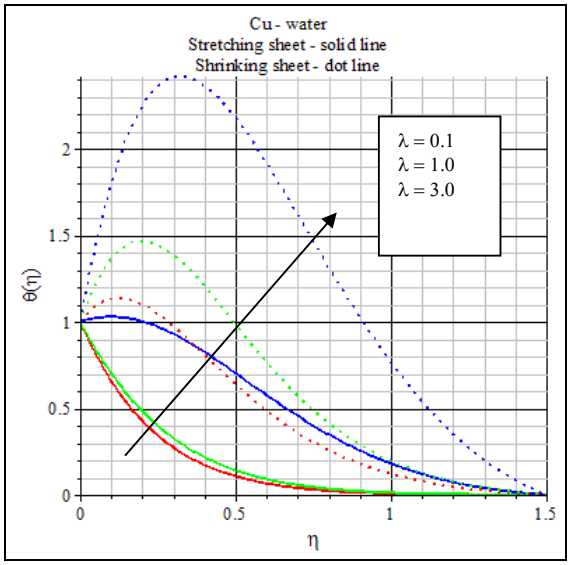

Fig 7(b)

Figs 7(a)-7(b): present the temperature profiles for different values of heat source parameter

Effect of heat source ($\lambda > 0$) on temperature distribution for stretching and shrinking sheet in the presence of base fluid (pure water) and nanofluid (Cu water) are shown in Figs. 7(a) and 7(b). Both stretching and shrinking sheet, it is observed that the temperature of the copper nanofluid increases with increase of heat source parameter. It is interesting to note that the heat source generates energy which causes the temperature of the fluid to increase in the Cu-water boundary layer for stretching and shrinking sheet. For pure water, it is predict that the temperature of the fluid initially increases and then decreases with increase of heat source for stretching sheet whereas the opposite effects are shown for shrinking sheet when $\eta \leq 0.385$ but beyond this value of ($\eta > 0.385$) the temperature increases with increase of heat source. Hence, the source plays an important role on controlling the thermal boundary layers quite effectively.

It is important to note that the temperature profiles for stretching sheet is lower than shrinking sheet with no peak formation for stretching sheet whereas the influence of internal heat generation on temperature distribution is more pronounced on the copper nanofluid than that of the base fluid for shrinking sheet. Increasing the heat source parameter $\lambda > 0$ has the tendency to increase the thermal state of the copper nanofluid. On the other hand, the presence of heat sink in the boundary layer absorbs energy which causes the temperature of the fluid to decrease. All these physical behavior are due to the combined effects of the strength of convective radiation and the size and shape of the nanoparticles in the nanofluid.

4. CONCLUSION

In this investigation, the effect of MHD laminar flow and heat transfer of copper nanofluid on a stagnation point flow and heat transfer over a porous stretching / shrinking sheet with variable stream conditions are analyzed. The governing partial differential equations are transformed into a set of nonlinear ordinary differential equations using similarity transformation and these equations are solved numerically using Maple 18 software. Following conclusions are drawn from the present study:

- In the presence of copper nanofluid, the temperature of the fluid is uniform for stretching sheet and decreases for shrinking sheet with increase of magnetic strength. These results clearly demonstrate that the magnetic field can be used as a means of controlling the flow and heat transfer characteristics.
- It is important to note that the temperature profile for shrinking sheet is higher to stretching sheet for copper nanofluids because the volume fraction of copper nanofluids in the presence of magnetic field raises the thermal conductivity and then the thermal boundary layer thickness increases.
- It is interesting to note that the increasing of thermal radiation on shrinking sheet plays a dominant role on temperature profiles compared to that of stretching sheet. This is because of improved thermal conductivity for specific volume concentration of copper nanoparticles.

- The temperature of the fluid gradually changes from higher value to lower value only when the strength of suction parameter higher than the magnetic strength in the presence of Cu-water for shrinking sheet because the copper nanofluid has high thermal conductivity whereas the temperature profiles for stretching sheet is lower than shrinking sheet and there is no peak formation for stretching sheet.
- Influence of internal heat generation on temperature distribution is more pronounced on the nanofluid than that of the base fluid for shrinking sheet. Increasing the heat source parameter $\lambda > 0$ has the tendency to increase the thermal state of the copper nanofluid.
- It is important to note that the increase of nano particle volume fraction ζ for shrinking sheet plays a dominant role on temperature field compared to that of stretching sheet.

Hence the fluid containing solid particles may significantly increase its conductivity. The flow over a continuously stretching / shrinking surface is an important problem in many engineering processes with applications in industries such as the hot rolling, wire drawing, paper production, glass blowing, plastic films drawing and glass-fiber production.

ACKNOWLEDGEMENT

The work was partly supported by University Tun Hussein Onn Malaysia, Johor, Malaysia, under the Fundamental Research Grant Scheme No. 1208/2013.

REFERENCES

[1] Y. Xuan, Q. Li,Investigation on convective heat transfer and flow features of nanofluids,J. Heat Transfer, 125 (2003), pp. 151–155

[2] J. Buongiorno, Convective transport in nanofluids, J. Heat Transfer, 128 (2006), pp. 240–250

[3] M.N. Pantzali, A.A. Mouza, S.V. Paras, Investigating the efficacy of nanofluids as coolants in plate heat exchangers (PHE), Chem. Eng. Sci., 64 (2009), pp. 3290–3300

[4] W. Duangthongsuk, S. Wongwises, Heat transfer enhancement and pressure drop characteristics of TiO_2–water nanofluid in a double-tube counter flow heat exchanger, Int. J. Heat Mass Transfer, 52 (2009), pp. 2059–2067

[5] N.S. Akbar, S. Nadeem, R. Ul Haq, Z.H. Khan, Radiation effects on MHD stagnation point flow of nano fluid towards a stretching surface with convective boundary condition, Chin. J. Aeronaut., 26 (6) (2013), pp. 1389–1397

[6] S. Nadeem, R. Ul Haq, Z.H. Khan, Heat transfer analysis of water-based nanofluid over an exponentially stretching sheet, Alexandria Eng. J., 53 (2014), pp. 219–224

[7] [X. Wang, A.S. Mujumdar, A review on nanofluids. Part I: Theoretical and numerical investigation, Braz. J. Chem. Eng. 25 (04) (2008) 613–630

[8] A.V. Kuznetsov, D.A. Nield, Natural convective boundary – layer flow of a nanofluid past a vertical plate, Int. J. Therm. Sci. 49 (2010) 243–247

[9] J.A. Eastman, S.U.S. Choi, S. Li, W. Yu, L.J. Thompson, Anomalously increased effective thermal conductivity of ethylene glycol – based nanofluids containing copper nanoparticles, Appl. Phys. Lett. 78 (6) (2001) 718–720

[10] M. Mostafa, T. Hayat, I. Pop, S. Asghar, S. Obaidat, Stagnation point flow of a nanofluid towards a stretching sheet, Int. J. Heat Mass Transfer 54 (2011) 5588–5594

[11] W.A. Khan, I. Pop, Boundary-layer flow of a nanofluid past a stretching sheet, Int. J. Heat Mass Transfer 53 (2010) 2477–2483

[12] W.A. Khan, A. Aziz, Natural convection flow of a nanofluid over a vertical plate with uniform surface heat flux, Int. J. Therm. Sci. 50 (2011) 1207–1214

[13] R. Nazar, M. Jaradat, M. Arifin, I. Pop, Stagnation-point flow past a shrinking sheet in a nanofluid, Cent. Eur. J. Phys. 9 (5) (2011) 1195–1202

[14] W. Ibrahim, B. Shankar, M.M. Nandeppanavar, MHD stagnation point flow and heat transfer due to nanofluid towards a stretching sheet, Int. J. Heat Mass Transfer 56 (2013) 1–9

[15] Oztrop and Abu-nada, Numerical study of natural convection in partially heated rectangular enclosures filled with nanofluids, Int. J. Heat Fluid Flow, 29 (2008) 1326–1336

[16] M.A.A. Hamad, I. Pop, Scaling transformations for boundary layer flow near the stagnation-point on a heated permeable stretching surface in a porous medium saturated with a nanofluid and heat generation/absorption effects, Trans. Porous Medium 87 (2010) 25–39

[17] T.R. Mahapatra, A.S. Gupta, Heat transfer in stagnation-point flow towards a stretching sheet, Heat Mass Transfer 38 (2002) 517–521

[18] Dulal Pal, Gopinath Mandal, K. Vajravelu, Flow and heat transfer of nanofluids at a stagnation point flow over a stretching/shrinking surface in a porous medium with thermal radiation, Applied Mathematics and Computation, 238(2014)208-224

APPENDIX A

```
>restart;
>with(plots) :
>Pr := 6.8; A := 0.5; S := 0.1; ϒ := 0.00; Ec := 0.1; Gr := 3.0; R := 1;
>M := 1.0; (n1) := 1; Z := 0.1; Ξ := 0.5; n := 0.5; λ := 0.5; N := 0.5;  K := 0.5; p := 0.5;
M := 1.0
n1 := 1
Z := 0.1
Ξ := 0.5
n := 0.5
λ := 0.5
N := 0.5
K := 0.5
p := 0.5
> (1 CT) := 0.5; (ρs) := 8933; (ρf) := 997.1; (cps) := 385; (cpf) := 4179; (ks) := 401; (kf)
      := 0.613; (βs) := 1.67E−5; (βf) := 21E−5;
>(Kfn) := (ks) + 2.(kf) − 2. ϒ.((kf) − (ks));
Kfn := 402.226
>(Kf) := (ks) + 2.(kf) + 2. ϒ.((kf) − (ks));
Kf := 402.226
>FNS := {f(η), u(η), v(η), h(η), w(η)} :

>
ODE := {diff(f(η), η) = u(η), diff(u(η), η) = v(η), diff(h(η), η) = w(η), diff(v(η), η)
   + (M + K).(A − u(η)) + Gr.h(η) + (1 − ϒ)^2.5.(1 − ϒ + ϒ.(ρs)/(ρf)).(A^2 + f(η)
   .v(η) − u(η)^2) = 0, diff(w(η), η) + Pr/(Kfn/Kf + N.(1 + (p − 1).h(η))^3).(3.N/Pr.(p
   − 1).(1 + (p − 1).h(η))^2.w(η)^2 + (1 − ϒ + ϒ.(ρs).(cps)/(ρf).(cpf)).(f(η).w(η) − 2.u(η)
   .h(η)) + λ.h(η) + Ec/(1 − ϒ)^2.5.v(η)^2) = 0};
```

$$ODE := \left\{ \frac{d}{d\eta} w(\eta) + 6.8 \left(\left(\frac{1}{1.000000000 + 0.5\,(1 - 0.5\,h(\eta))^3} \right).(-0.1102941176\,(((1 - 0.5\,h(\eta))^2).(w(\eta)^2)) + 1.\,(f(\eta).w(\eta)) - 2.\,(u(\eta).h(\eta)) + 0.5\,h(\eta) + 0.1\,v(\eta)^2) \right) = 0,\ \frac{d}{d\eta} v(\eta) + 1.00 - 1.5\,u(\eta) + 3.0\,h(\eta) + 1.\,(f(\eta).v(\eta)) - 1.\,u(\eta)^2 = 0,\ \frac{d}{d\eta} f(\eta) = u(\eta),\ \frac{d}{d\eta} h(\eta) = w(\eta),\ \frac{d}{d\eta} u(\eta) = v(\eta) \right\}$$

```
>IC := {f(0) = S, u(0) = R, h(0) = 1, v(0) = α, w(0) = β};
IC := {f(0) = 0.1, h(0) = 1, u(0) = 1, v(0) = α, w(0) = β}
>L := 1.5;
L := 1.5
>BC := {u(L) = A, h(L) = 0};
BC := {h(1.5) = 0, u(1.5) = 0.5}
>infolevel[shoot] := 1 :
>S := shoot(ODE, IC, BC, FNS, [α = 2.2564181646, β = -4.417289468]) :
shoot: Step # 1
shoot: Parameter values : alpha = 2.2564181646 beta = -4.417289468
shoot: Step # 2
shoot: Parameter values : alpha = HFloat(-0.03669255472238531) beta = HFloat(-5.083482444053297)
shoot: Step # 3
shoot: Parameter values : alpha = HFloat(-0.5142709052045595) beta = HFloat(-4.262246620880692)
shoot: Step # 4
shoot: Parameter values : alpha = HFloat(-0.421823145377327) beta = HFloat(-3.9284798110446237)
shoot: Step # 5
shoot: Parameter values : alpha = HFloat(-0.42120120144630296) beta = HFloat(-3.939486849799802)
shoot: Step # 6
shoot: Parameter values : alpha = HFloat(-0.42117539406290083) beta = HFloat(-3.9394413453483375)
```